Available online at www.sciencedirect.com

ScienceDirect

Mendeleev Commun., 2019, **29**, 489–491

Mendeleev Communications

Structure and quantum chemical study of crystalline platinum(II) acetate

Alexander A. Markov,*[a] Ilya A. Yakushev,[a] Andrey V. Churakov,[a] Victor N. Khrustalev,[b,c] Natalia V. Cherkashina,[a] Igor P. Stolarov,[a] Alexander E. Gekhman[a] and Michael N. Vargaftik[a]

[a] *N. S. Kurnakov Institute of General and Inorganic Chemistry, Russian Academy of Sciences, 119991 Moscow, Russian Federation. Fax: +7 495 954 1279; e-mail: hello@sasha-markov.net*

[b] *Peoples Friendship University of Russia (RUDN University), 117198 Moscow, Russian Federation*

[c] *National Research Center 'Kurchatov Institute', 123182 Moscow, Russian Federation*

DOI: 10.1016/j.mencom.2019.09.003

Calculations by the hybrid functional PBE0 with scalar relativistic corrections and the QTAIM method revealed the metal–metal bonding in the molecule of platinum(II) acetate $Pt_4(\mu\text{-}OAc)_8$, which stabilizes the molecule by 50 kcal mol^{-1}.

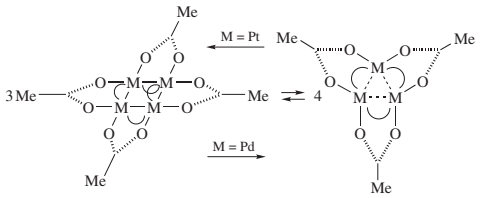

It is well known that the carboxylate complexes of platinum(II) and palladium(II), which are widely used in coordination chemistry, have different molecular structures. For instance, platinum(II) acetate $Pt_4(\mu\text{-}OAc)_8$ **1** has a slightly distorted square metal skeleton and very short (2.495 Å) Pt–Pt distances,[1–3] while $Pd_3(\mu\text{-}OAc)_6$ is a triangle with much longer (3.1–3.2 Å) Pd–Pd distances.[4,5] The reason for this difference was not exactly understood.

The electronic structure of $Pd_3(\mu\text{-}OAc)_6$ has been studied comprehensively,[6,7] whereas chemical bonding in the molecule of $Pt_4(\mu\text{-}OAc)_8$ was examined only by semiqualitative EHMO calculations.[8] This fact inspired us to investigate the electronic structure of $Pt_4(\mu\text{-}OAc)_8$ in detail by the hybrid functional PBE0[9] with scalar relativistic corrections and the QTAIM theory.[10] This approach makes it possible to evaluate a decrease in energy caused by bonding and electron density distribution in the molecule.

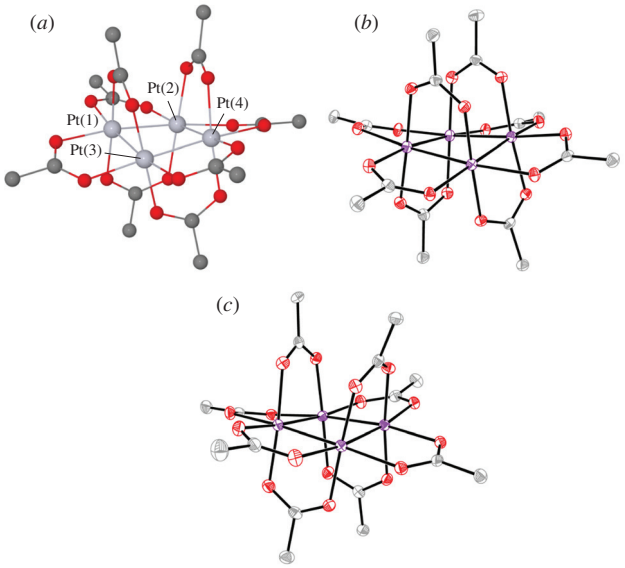

Figure 1 (*a*) Calculated equilibrium molecular structure of $Pt_4(\mu\text{-}OAc)_8$, (*b*, *c*) molecular structures of $Pt_4(\mu\text{-}OAc)_8$ from solvent-free crystals and benzene solvate (**1** and **2**, respectively) [Pt–Pt 2.4870(5)–2.4970(6) Å, Pt–O 1.995(5)–2.185(5) Å, thermal ellipsoids drawn at a 30% probability level]. Hydrogen atoms are omitted for clarity.

To compare the results of our calculations (the molecular geometry of **1**) with experimental data, we prepared the samples of crystalline **1** by different protocols (because the preparation of platinum(II) acetate by a classical method[11] is poorly reproducible) and determined their structure by single-crystal X-ray diffraction analysis. Previous attempts to improve synthetic approaches (for instance, by the metathesis of platinum(II) chloride with silver acetate)[12] afforded crystalline platinum(II) acetate in an insufficient yield (at most 47% but with a suspiciously blue color),[12] being contaminated with non-crystalline blue to brown by-products,[13–18] apparently, the platinum acetate blue containing Pt in intermediate oxidation states between II and III.[19]

In this work, we prepared the crystals of **1** for XRD experiments by two protocols: (1) a reaction of platinum acetate blue $Pt(OAc)_{2.5}$ or $Pt(OAc)_{2.75}$ (PAB)[13] with manganese acetate $Mn(OAc)_2 \cdot 4H_2O$,† and (2) the cation exchange of $K_2[Pt(OAc)_4] \cdot 6AcOH$ or $Cs_2[Pt(OAc)_4] \cdot 6AcOH$ on a column with KU-2 cation-exchange resin in the acidic form.‡ As a result, we obtained the crystalline specimens of both the known platinum(II) acetate $Pt_4(OAc)_8$

† *One-stage synthesis of* **1** (*protocol 1*). The platinum acetate blue (PAB) of composition $Pt(OAc)_{2.5}$ (134.5 mg, 392 mmol) and $Mn(OAc)_2 \cdot 4H_2O$ (115 mg, 465 mmol) were stirred in glacial acetic acid (30 ml) at 95 °C for 30 h to produce the platinum(II) acetate $Pt_4(OAc)_8$ **1** (37 mg, 30% based on Pt) along with the heterometallic complex $Pt_2Mn_2(OAc)_8 \cdot 2C_6H_6$ (23.3 mg, 10.5% based on Pt).

One-stage synthesis of **2** (*protocol 1*). Another synthesis starting from the platinum acetate blue of composition $Pt(MeCOO)_{2.75}$ (259 mg, 724 mmol) and $Mn(OAc)_2 \cdot 4H_2O$ (355 mg, 1450 mmol) in 50 ml of glacial acetic acid (2.5 h at 97 °C) produced the benzene crystal solvate platinum(II) acetate $Pt_4(OAc)_8 \cdot 2.6C_6H_6$ **2** (26 mg, 12% based on Pt) along with the Pt–Mn heterometallic complex. See details in Online Supplementary Materials.

‡ *Two-stage synthesis of* **1** *and* **2**. The synthesis was performed analogously to that of $Pt^{II}(\mu\text{-}OAc)_4M^{II}(AcOH)_4$ (M = Ca, Sr, Ba).[14] (*1*) A mixture of $PtO_2 \cdot 4H_2O$ (152.8 mg, 0.51 mmol) and KOAc (128.3 mg, 1.30 mmol) was refluxed in 20 ml of glacial acetic acid for 3 h to give $K_2[Pt(OAc)_4] \cdot 6AcOH$ (330.9 mg, 75% based on Pt). Analogously $Cs_2[Pt(OAc)_4] \cdot 6AcOH$ was prepared in 71% yield (based on Pt). (*2*) A solution of $K_2[Pt(OAc)_4] \cdot 6AcOH$

[Figure 1(*b*)] and a new crystal solvate of platinum(II) acetate with benzene 5 $Pt_4(OAc)_8 \cdot 13C_6H_6$ **2** [Figure 1(*c*)].

The X-ray crystallography experiments[§] showed good agreement between our data for the newly prepared crystals of **1** and those for published ones[1–3] except for the thermal parameters that were not earlier examined.[1–3] The crystal of **1** is monoclinic, space group $P2_1/c$, $V = 2466.3(9)$ Å^3. Four platinum atoms form a rectangular framework linked by acetate ligands [see Figure 1(*b*)], so that each platinum atom is located in an octahedral environment. Four platinum atoms form a slightly distorted square framework with Pt–Pt distances of 2.4870(5)–2.4970(6) Å and angles of 88.793(18)–89.903(17)°; the mean deviation of Pt atoms from the plane Pt(1)–Pt(2)–Pt(3)–Pt(4) is 0.1265(3) Å. The axial and equatorial bridging acetate groups are nonequivalent: the axial oxygen atoms are spaced from Pt at shorter distances [1.995(5)–2.018(5) Å] than the equatorial O atoms [2.141(4)–2.185(5) Å] (Table S1, see Online Supplementary Materials).

The monoclinic crystal of solvated complex **2** has the space group $C2/c$ and large unit cell volume $V = 19224(8)$ Å^3. The main interatomic distances in platinum(II) acetate molecules are close to those in a crystal of **1** with the same geometrical parameters. The solvation benzene molecules are weakly bound to each other and the Pt_4 units.

DFT calculations[¶] with scalar relativistic corrections yielded the equilibrium geometrical parameters of $Pt_4(\mu\text{-}OAc)_8$ **1**, which are consistent with XRD data (Table S3). Calculated at *Rel* level values of tetramer/trimer equilibrium (Scheme 1), 64.5 kcal mol^{-1}, and the dissociation energy of **1** relative to two dimers, 69.6 kcal mol^{-1}, confirm the stability of tetrameric platinum acetate.

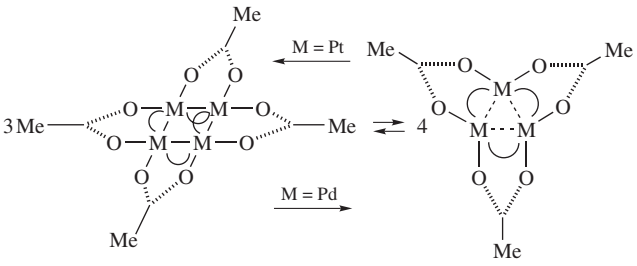

Scheme 1 Trimer/tetramer equilibrium for platinum and palladium acetates. Some acetate bridges shown as ∩ for clarity.

We determined that QTAIM delocalization index [δ(A,B), the number of electron pairs delocalized between two atoms] in $Pt_4(\mu\text{-}OAc)_8$ is larger for Pt–Pt interactions (0.90, Table 1) than for bridging Pt–O (0.72 for the axial and 0.52 for equatorial acetates). The difference between axial and equatorial delocalization indices correlates with the observation that equatorial ligands are easier to substitute compared to axial ones.[8]

In the calculations, in addition to the equilibrium molecular structure of crystalline **1**, we found another equilibrium structure **1a** [Figure 2(*b*)] characterized by long *R*(Pt–Pt) of 3.234 and 3.727 Å (Table S4), small δ(Pt,Pt) of 0.20 and 0.06 (Table 1), and an almost square-planar environment of platinum atoms. Considering that **1** lies lower in energy than **1a** by 50.1 kcal mol^{-1} (Table 2) and two isoelectronic complexes mainly differ in Pt–Pt interactions [four atomic pairs with δ(Pt,Pt) = 0.90 in **1** but only two with δ(Pt,Pt) = 0.20 in **1a**], we can conclude that the Pt–Pt interaction in **1** is stabilizing.

By analogy with platinum acetates **1** and **1a**, we calculated the equilibrium geometries of tetranuclear palladium acetates **3** and **3a** (Figure 2). We found that the structure of **3** with a short distance *R*(Pd–Pd) lies significantly higher in energy (by 22.2 kcal mol^{-1}, see Table 2) than the structure of **3a** with long *R*(Pd–Pd). Note that, despite almost equal metal–ligand and metal–metal distances, platinum and palladium complexes differ in delocalization indices, namely, δ(Pt,O) and δ(Pt,Pt) are larger than δ(Pd,O) and δ(Pd,Pd), respectively (see Table 1). This may be a sign of stronger metal–metal and metal–ligand interactions in platinum acetates.

Hence, based on the calculated values of energy and delocalization index, we concluded that (1) metal–metal and metal–equatorial ligand interactions in tetranuclear platinum and palladium acetates are concurrent interactions; (2) Pt–Pt interaction in platinum(II) complex **1** is stabilizing, whereas Pd–Pd in hypothetic tetranuclear

Table 1 Mean electron delocalization indices in platinum and palladium acetates obtained at *Rel* computational level. Standard deviations are shown in parentheses.

Complex	<δ(M,M)>	<δ(M,O)>	<δ(C,O)>	<δ(C,C)>
$Pt_4(\mu\text{-}OOCMe)_8$ **1**	0.902			
equatorial acetates		0.522(5)	1.050(4)	0.904
axial acetates		0.715(9)	1.017(2)	0.917
$Pd_4(\mu\text{-}OOCMe)_8$ **3**	0.716			
equatorial acetates		0.412(4), 0.504(4)	1.051(17)	0.903
axial acetates		0.635(11)	1.020(2)	0.914
$Pd_3(\mu\text{-}OOCMe)_6$	0.128(9)	0.632(10)	1.034(3)	0.904(1)
$Pt_4(\mu\text{-}OOCMe)_8$ **1a**	0.205, 0.058	0.708(14)	1.022(6)	0.910(2)
$Pd_4(\mu\text{-}OOCMe)_8$ **3a**	0.124, 0.035	0.623(10)	1.030(4)	0.905(2)

or $Cs_2[Pt(OAc)_4] \cdot 6AcOH$ in glacial acetic acid was flown through a column with the acidic form of cation exchange resin KU-2, eluent glacial acetic acid to produce **1** (yield 28–30% based on Pt) and the benzene solvate **2** (yield 20% based on Pt). See details in Online Supplementary Materials.

[§] X-ray diffraction data for both **1** and **2** were collected on the 'Belok' beamline of the Kurchatov Synchrotron Radiation Source (National Research Center 'Kurchatov Institute', Moscow, Russian Federation) in the φ-scan mode using a Rayonix SX165 CCD detector. The structures were solved by direct methods and refined by full-matrix least-squares on F^2 with anisotropic displacement parameters for all non-hydrogen atoms. See details in Online Supplementaty Materials.

Crystal data for **1**. Red prism (0.10×0.05×0.05 mm), monoclinic, space group $P2_1/c$, at 100 K: $a = 11.943(2)$, $b = 10.607(2)$ and $c = 19.479(4)$ Å, $\beta = 91.92(3)°$, $V = 2466.3(9)$ Å^3, $Z = 4$, $d_{calc} = 3.374$ g cm^{-3}, $M_w = 1252.71$. 38499 reflections were collected ($1.891° < \theta < 30.767°$), absorption coefficient $\mu = 29.440$ mm^{-1}. Data/restraints/parameters: 5633/0/334. 5633 independent reflections ($R_{int} = 0.0414$) and 5403 with $I > 2\sigma(I)$. The final refinement parameters were: $R_1 = 0.0303$, $wR_2 = 0.0808$ for reflections with $I > 2\sigma(I)$; $R_1 = 0.0315$, $wR_2 = 0.0816$ for all reflections; extinction coefficient 0.00142(8); largest diff. peak/hole 1.801/–2.019 eÅ^{-3}. GOF = 1.086.

Crystal data for **2**. Red prism (0.15×0.12×0.08 mm), monoclinic, space group $C2/c$, at 100 K: $a = 50.081(10)$, $b = 14.858(3)$ and $c = 29.537(6)$ Å, $\beta = 118.99(3)°$, $V = 19224(8)$ Å^3, $Z = 4$, $d_{calc} = 2.515$ g cm^{-3}, $M_w = 7278.95$. 120947 reflections were collected ($1.538° < \theta < 27.999°$), absorption coefficient $\mu = 18.847$ mm^{-1}. Data/restraints/parameters: 17085/43/1288. 17085 independent reflections ($R_{int} = 0.0687$) and 14340 with $I > 2\sigma(I)$. The final refinement parameters were: $R_1 = 0.0298$, $wR_2 = 0.0707$ for reflections with $I > 2\sigma(I)$; $R_1 = 0.0397$, $wR_2 = 0.0752$ for all reflections; extinction coefficient 0.0000275(16), largest diff. peak/hole 1.502/–1.832 eÅ^{-3}. GOF = 1.011.

CCDC 1874439 and 1896898 contain the supplementary crystallographic data for this paper. These data can be obtained free of charge from The Cambridge Crystallographic Data Centre *via* http://www.ccdc.cam.ac.uk.

[¶] *Computational details*. We performed spin-restricted calculations with hybrid PBE0 functional using GAMESS-US package[20] at four computational levels: non-relativistic calculations (*NR*) with all electron DZP basis for palladium, mDZP basis for platinum, and def2-SVP basis for light atoms; with metal core potential (*MCP*) and scalar relativistic corrections using IMCP SR1 basis; relativistic calculations (*Rel*) at the 3rd order Douglas–Kroll–Hess level with all electron Sapporo-DKH3-DZP-2012 basis; single point calculations (*Rel/sp*) at *Rel* geometry with additional diffuse *sp* functions. Geometry optimizations at *Rel* level performed with OPTTOL parameter set to 0.005. The wave functions obtained at *Rel* level were used in QTAIM analysis with the AIMAll package.[21] Fileset containing all calculated equilibrium geometries was deposited on figshare.[22]

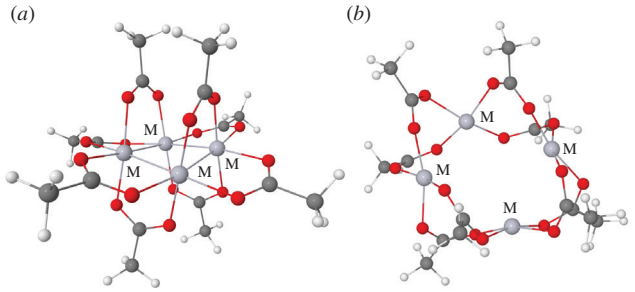

Figure 2 Equilibrium structures of $M_4(\mu\text{-}OAc)_8$ with (*a*) short M = Pt (**1**), Pd (**3**) and (*b*) long M–M distances M = Pt (**1a**), Pd (**3a**). Files containing optimized coordinates are available for downloading from ref. 22.

Table 2 Difference in total electronic energy between **1** and **1a** or **3** and **3a** ($\Delta E = E_{short} - E_{long}$), calculated at various computational levels.

	ΔE / kcal mol^{-1}	
	Pt	Pd
NR	–59.7	–64.3[a]
MCP	–23.2	30.7
Rel	–52.7	22.1
Rel/sp	–50.1	22.2

[a] The discrepancy caused by very different optimized geometry at the *NR* level and other methods (Table S4).

complex **3** of palladium(II) is not despite very similar metal–metal distances; and (3) the energy difference between **1** and **1a**, 50.1 kcal mol^{-1}, is mainly due to Pt–Pt bonding. These findings give a clue to the general pattern of bonding in the chemistry of polynuclear platinum and palladium compounds.

This work was supported by the Russian Science Foundation (project no. 18-73-10206) and performed using the equipment of the JRC PMR at the Institute of General and Inorganic Chemistry, Russian Academy of Sciences.

Online Supplementary Materials

Supplementary data associated with this article can be found in the online version at doi: 10.1016/j.mencom.2019.09.003.

References

1 M. A. A. F. de C. T. Carrondo and A. C. Skapski, *J. Chem. Soc., Chem. Commun.*, 1976, 410.
2 M. A. A. F. de C. T. Carrondo and A. C. Skapski, *Acta Crystallogr., Sect. B*, 1978, **34**, 1857.
3 M. A. A. F. de C. T. Carrondo and A. C. Skapski, *Acta Crystallogr., Sect. B*, 1978, **34**, 3576.
4 A. C. Skapski and M. L. Smart, *J. Chem. Soc. D*, 1970, 658.
5 F. A. Cotton and S. Han, *Rev. Chim. Miner.*, 1985, **22**, 277.
6 B. E. Haines, J. F. Berry, J.-Q. Yu and D. G. Musaev, *ACS Catal.*, 2016, **6**, 829.
7 R. J. Pakula, M. Srebro-Hooper, C. G. Fry, H. J. Reich, J. Autschbach and J. F. Berry, *Inorg. Chem.*, 2018, **57**, 8046.
8 T. Yamaguchi, Y. Sasaki, A. Nagasawa, T. Ito, N. Koga and K. Morokuma, *Inorg. Chem.*, 1989, **28**, 4311.
9 C. Adamo and V. Barone, *J. Chem. Phys.*, 1999, **110**, 6158.
10 R. F. W. Bader, *Atoms in Molecules: A Quantum Theory*, Oxford University Press, Oxford, 1990.
11 T. A. Stephenson, S. M. Morehouse, A. R. Powell, J. P. Heffer and G. Wilkinson, *J. Chem. Soc.*, 1965, 3632.
12 M. Basato, A. Biffis, G. Martinati, C. Tubaro, A. Venzo, P. Ganis and F. Benetollo, *Inorg. Chim. Acta*, 2003, **355**, 399.
13 J. M. Davidson and C. Triggs, *Chem. Ind. (London)*, 1966, 306.
14 I. P. Stolarov, I. A. Yakushev, P. V. Dorovatovskii, Ya. V. Zubavichus, V. N. Khrustalev and M. N. Vargaftik, *Mendeleev Commun.*, 2018, **28**, 200.
15 R. I. Rudy, N. V. Cherkashina, G. Ya. Mazo, Ya. V. Salyn' and I. I. Moiseev, *Bull. Acad. Sci. USSR, Div. Chem. Sci.*, 1980, **29**, 510 (*Izv. Akad. Nauk SSSR, Ser. Khim.*, 1980, 754).
16 D. Wright, *GB Patent 1214552 (A1)*, 1970.
17 H. Kunkely and A. Vogler, *Inorg. Chem. Commun.*, 2000, **3**, 594.
18 T. Ramstad and J. D. Woollins, *Transition Met. Chem.*, 1985, **10**, 153.
19 N. V. Cherkashina, D. I. Kochubey, V. V. Kanazhevskiy, V. I. Zaikovskii, V. K. Ivanov, A. A. Markov, A. P. Klyagina, Z. V. Dobrokhotova, N. Y. Kozitsyna, I. B. Baranovsky, O. G. Ellert, N. N. Efimov, S. E. Nefedov, V. M. Novotortsev, M. N. Vargaftik and I. I. Moiseev, *Inorg. Chem.*, 2014, **53**, 8397.
20 M. W. Schmidt, K. K. Baldridge, J. A. Boatz, S. T. Elbert, M. S. Gordon, J. H. Jensen, S. Koseki, N. Matsunaga, K. A. Nguyen, S. Su, T. L. Windus, M. Dupuis and J. A. Montgomery, Jr., *J. Comput. Chem.*, 1993, **14**, 1347.
21 T. A. Keith, *AIMAll*, *Version 17.11.14*, TK Gristmill Software, Overland Park, KS, USA, 2017 (aim.tkgristmill.com).
22 A. A. Markov, *Figshare*, 2019, DOI: 10.6084/m9.figshare.7938170.

Received: 13th March 2019; Com. 19/5849